

Ionic radius effect on structural and electrical properties of barium strontium titanate thin films

Hamed. A. Gatea^{a,*}, Maithm. A. Obaid^b, Abdulkareem. M. Mohammed^c

^a*Department of Medical Physics, College of Applied Medical Science, Shatrah University, Thi-Qar, 64001, Iraq*

^b*Department of Medical Physics, College of Applied Medical Science, Shatrah University, Thi-Qar, 64001, Iraq*

^c*College of Pharmacy, National University of Science and Technology, Dhi Qar, 64001, Iraq*

The effect of ion radius on the structural and electrical properties of the perovskite oxide Ba_{1-x}Sr_xTiO₃ thin film is investigated in this work. X-ray diffraction analysis confirmed the formation of phase perovskite structures. Investigations of ceramic microstructures and mechanical properties showed their dependence on the value of ratio x. X-ray diffraction (XRD) and Field emission scanning electron microscopy (FESEM) are used to study the crystallographic aspects of the materials. The XRD pattern changed from tetragonal to cubic as x rose. FESEM images revealed the particle size varied with the values of x increased. The results show that as the ion radius varies, the crystal structure undergoes distortions, affecting the symmetry and stability of the BaSrTiO₃ thin films. Electrical properties change depending on the change in particle size.

(Received April 6, 2024; Accepted July 26, 2024)

Keywords: BST films, Electrical properties, FESEM, Barium strontium titanate oxide, Conductivity

1. Introduction

BST thin films are chosen over their bulk equivalents for more applications, such as phase shifters, solar cells, varactors, and tunable microwaves[1]. Thin films are used to manufacture devices, due to the small size and light weight of the films [2][3]. The dielectric properties of thin films are different between bulk and film. The dielectric constant of BST bulk matter is much higher than BST thin film. There is a correlation between the thickness of the layer and the dielectric constant. [4]. The values of the dielectric constant rely on the film thickness; they vary with some elements such as composition, substrate temperature, sintering temperature, thin-film annealing, and grain size influence.[5][6].

We have created a prototype BST capacitor using a metal-insulator-metal (MIM) structure, with silver serving as the electrodes on both the top and bottom. This capacitor's BST material is in the manometer range.[7]. A thin-film capacitor made of barium strontium titanate was created on Si surfaces that had metals on them.[8][9].

Barium strontium titanate is a perovskite oxide material with the general chemical formula (Ba_{1-x}Sr_xTiO₃), where Ba and Sr are the alkaline earth metal ions, and Ti is the transition metal ion[10]. Barium Strontium Titanate (BST) is a well-known perovskite material that exhibits interesting electrical properties, making it suitable for various applications such as dielectric capacitors, ferroelectric devices, and as a material in thin-film transistors. The electrical conductivity of BST thin films can be affected by various factors, including the ion radius of the constituent elements[11][12].

Ba_{1-x}Sr_xTiO₃ is a solid solution of Barium and Strontium Titanate (SrTiO₃, BaTiO₃), where the value of x represents the fraction of SrTiO₃ in the mixture[13]. As the value of x varies, the lattice structure, crystallographic phases, and physical properties of the material may change,

* Corresponding author: hamedalwan14@gmail.com
<https://doi.org/10.15251/DJNB.2024.193.1117>

which could affect the porosity in complex ways. $Ba_{1-x}Sr_xTiO_3$ is a solid solution compound formed by substituting strontium (Sr) for barium (Ba) in the crystal structure of barium titanate ($BaTiO_3$). The conductivity of $Ba_{1-x}Sr_xTiO_3$ can vary with different values of the substitution ratio x [14][15].

The electrical conductivity of a material is influenced by its chemical composition, and in the case of solid solutions like $Ba_{1-x}Sr_xTiO_3$ (BST), it depends on the molar fraction (x) of strontium (Sr) in the compound. BST is a well-known perovskite oxide with various applications, particularly in thin film form for electronic devices like capacitors, memory elements, and tunable microwave devices[16].

At low values of x (e.g., $x = 0.2$), the conductivity of $Ba_{1-x}Sr_xTiO_3$ may be relatively low. As x increases, the number of Sr ions in the crystal lattice increases, resulting in an increased concentration of charge carriers. This higher concentration of charge carriers enhances the material's electrical conductivity[2][17]. As x continues to increase (e.g., $x = 0.6$), the conductivity of $Ba_{1-x}Sr_xTiO_3$ can reach even higher levels. Therefore, the conductivity behavior may become more complex, influenced by factors such as the formation of secondary phases or structural changes[18].

The porosity changes with the range of x ratio ($x = 0.2$ to $x = 0.6$) for the material $Ba_{1-x}Sr_xTiO_3$ cannot be determined solely based on the information provided [4]. The reason is that the porosity of $Ba_{1-x}Sr_xTiO_3$ is not solely dependent on the value of x , but it is also influenced by other factors, such as the preparation method, sintering conditions, and any potential additives or impurities[19]. By carefully controlling the Sr content, it is possible to tailor the properties of BST thin films for various applications[20].

The ionic radii of Ba^{2+} , Sr^{2+} , and Ti^{4+} ions are systematically varied in this study to understand their impact on the crystal structure and electrical behavior of $BaSrTiO_3$. This work sheds light on the relationship between ion radius on the structural and electrical characteristics of $BaSrTiO_3$, laying the groundwork for customizing perovskite oxide properties for technological uses.

2. Experimental details

The raw materials starting to prepare the $Ba_{1-x}Sr_xTiO_3$ compound consist of strontium, barium acetate, and titanium isopropoxide. The required amount of Ba acetate ($(Ba(CH_3COO)_2)$) and Sr acetate ($(Sr(CH_3COO)_2)$) is weighted according to the desired composition of BST. Dissolve the amount (Ba, Sr acetate) in acetic acid. The mixture solution was stirred on the magnetic stirrer until dissolved completely. Add stabilizer structure to titanium isopropoxide ($Ti(OC_3H_7)_4$) to maintain its structure. The solution is heated at a low temperature of $60^\circ C$ to evaporate excess solvent until a clear gel-like solution is obtained. Add a few drops of ammonium hydroxide to the solution to adjust the PH around 4.5-5.

The substrate is cleaned in ethanol and deionized water by ultra-sonication. The nitrogen gas is used to dry or by air. Sometimes, add a small amount of PVA and Triton to improve the film adhesion and uniformity. The substrate on the spin coater chuck and secure it. Stir the solution to ensure homogeneous dispersion. The sol-gel is poured onto the substrate, and the spin coater starts at low speed (500-1000) for a few seconds to spread the solution uniformly. Increase the spin speed (e.g., 2000-4000 rpm) for a desired duration to achieve the desired film thickness. After the annealing process, allow the furnace to cool down to room temperature naturally.

The specific parameters such as spin coating speed, solution concentration, film thickness, time, and annealing temperature should be optimized based on your specific requirements and the properties you aim to achieve in the BST thin film.

3. Characterization

Cu Ka ($k = 1.54056 \text{ \AA}$) energy at 40 kV and 40 mA was used for X-ray powder diffraction (XRD). Scanning electron microscopy (FESEM, JSM EMP-800, JEOL, Japan) was used to see the nanostructures. An LCR meter (HP4284A, Agilent, Palo Alto, CA) was used to look at how the dielectric properties change with frequency and temperature. The JASCO V-570 spectrophotometer

is a UV–UV–VIS–NIR scanning spectrophotometer that is used to study optical qualities. XRD (Bruker, Germany) with Cu K α (40 kV and 30 mA) was used to look at the ferroelectric samples. A Field emission Scanning Electron Microscope (FESEM, S-4700, Hitachi) was used to look at the ferroelectric sample's grain size and particle size. An impedance analyzer, LCR, was used to test the electric properties.

4. Theoretical part

Using information and Debye-Schere's formula, the average crystallite size (t) was calculated: [4]

$$D = \frac{0.9\lambda}{\beta \cos\theta} \quad (1)[4]$$

λ is the X-ray wavelength (0.1540 nm), D is the crystallite size, and β (FWHM) is the full width at half-maximum [12].

The lattice parameters (a and c) for samples were determined from XRD data based on the tetragonal phase using the following relation, with a precision of $\pm 0.002 \text{ \AA}$: [4]

$$\frac{1}{d^2} = \frac{h^2+k^2}{a^2} + \frac{l^2}{c^2} \quad (3) [4]$$

where a and c are the lattice parameters, d is the inter-planar spacing, and (hkl) are Miller indices [12].

The cubic phase is as follows:

$$a = d\sqrt{(h^2 + k^2 + l^2)} \quad (4) [4]$$

The dielectric materials are insulator materials with high dielectric permittivity. The material's ability to store an electric charge is described as its dielectric constant. The more factors affect the capacitance of the medium, such as shape, size, and relative permittivity ϵ_r :

$$C = \epsilon_r \frac{A}{d} \quad (5)[4]$$

where C stands for the capacitance of the material, (A) signifies the area of the capacitive cell, and (d) indicates its thickness" [8].

A lot of the time, the relative dielectric permittivity is used to measure how a barrier material reacts to an electric field. What it means is: [4]

$$\epsilon_r = \frac{\epsilon_0}{\epsilon_s} \quad (6)[4]$$

where (ϵ_s) stands for the static permittivity of the material and (ϵ_0) indicates the vacuum permittivity."

The following equations typically quantify the dissipation factor, which is the decrease in the dielectric constant:[12]

$$\tan\theta = \frac{\text{imaginary part}}{\text{real part}} \quad (7) [4]$$

The electrical conductivity can be inferred from the dielectric data using the following correlation:

$$\sigma = 2\pi f \epsilon_0 \epsilon \quad (8) [12]$$

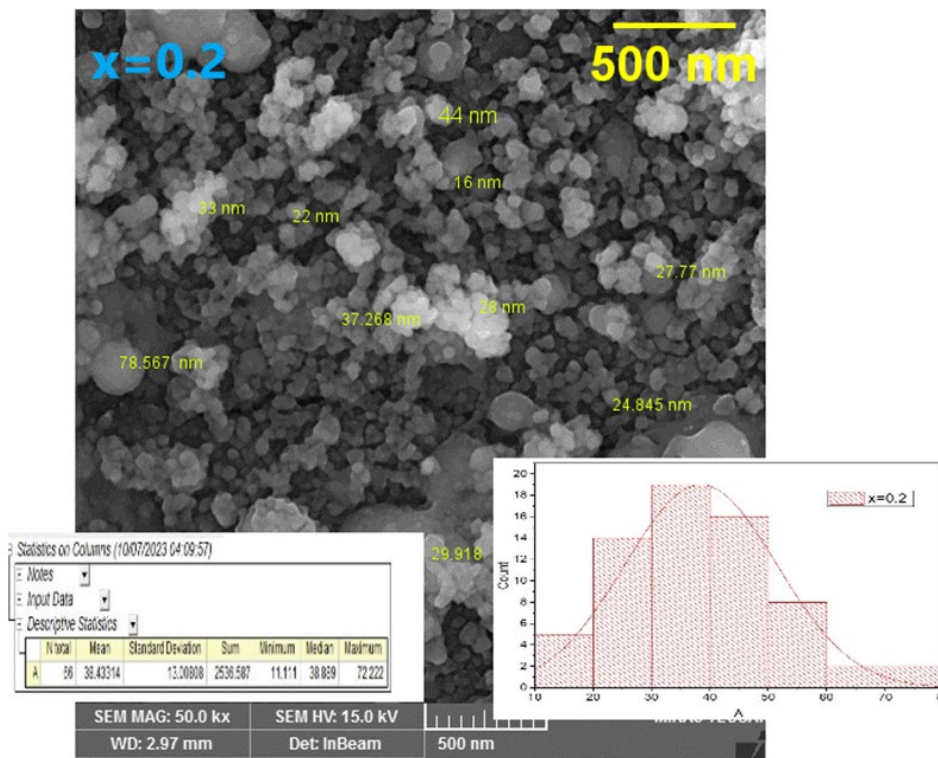
where f is the frequency (Hz), ϵ_0 is the permittivity of vacuum (8.854×10^{-12} F/m) and ϵ is the imaginary part of the dielectric permittivity.

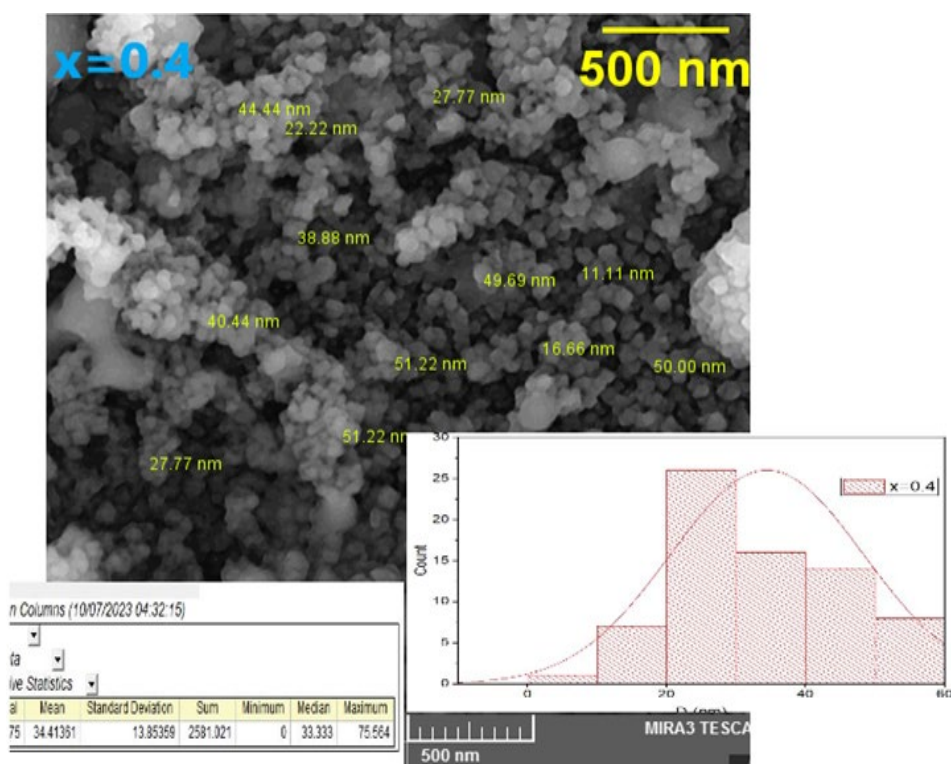
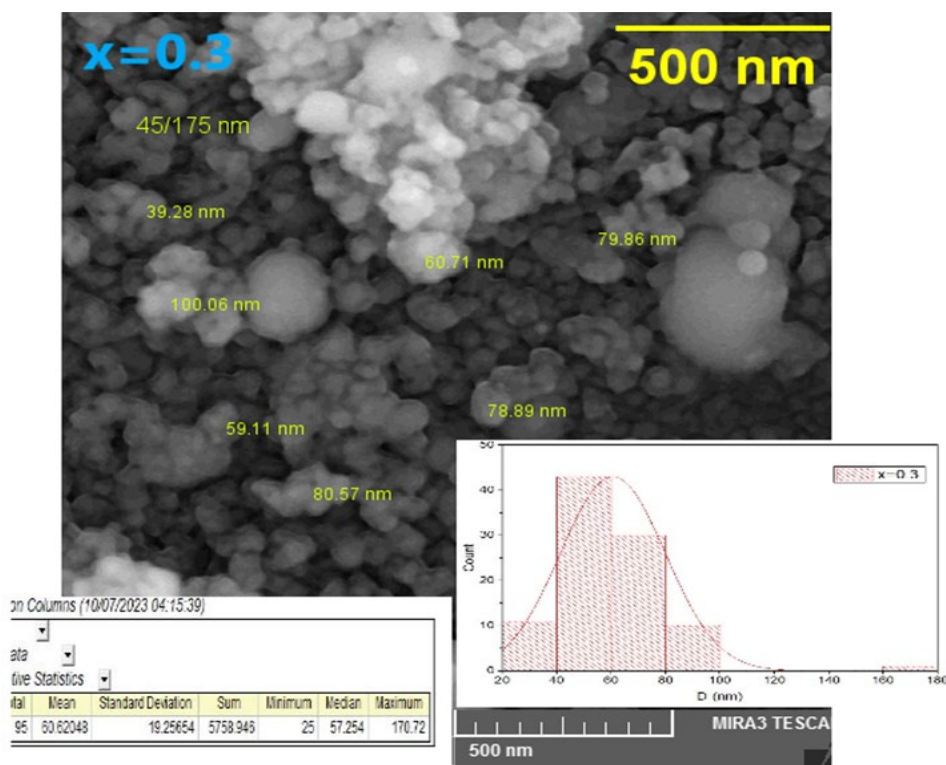
5. Results and discussion

Fig. 1 shows, the ratio of x influences the lattice parameters and crystal structure of BST. As the Sr^{+2} content increases (higher ' x ' ratio), it introduces lattice strain due to the difference in ionic radii between Ba^{2+} and Sr^{2+} . This strain can affect the surface morphology, leading to changes in grain boundaries, defects, and surface roughness. These defects can affect the morphology and properties of the surface, such as charge trapping, leakage current, and dielectric response. The Ba/Sr ratio influences the surface smoothness of BST films. Generally, higher Sr^{+2} content tends to promote a smoother film surface. The presence of Sr^{+2} in the thin film composition can result in reduced surface roughness, leading to improved film quality and enhanced device performance. Increased roughness can affect the electrical, optical, and mechanical properties of the material.

The Ba/Sr ratio can induce strain in the thin film due to the difference in ionic radii between Ba and Sr ions. This strain can influence the formation of defects and dislocations, which, in turn, affect the surface morphology. Higher strain levels can lead to an increased density of defects and a rougher surface. It is important to note that the specific effects of the Ba/Sr ratio on surface morphology may also depend on other growth parameters, such as deposition technique, substrate type, and annealing conditions. Experimental optimization of the Ba/Sr ratio, along with these parameters, can help achieve desired surface morphologies for specific applications in electronic devices, such as capacitors, memories, and sensors.

The presence of porosity can significantly affect the surface morphology, introducing voids or irregular features on the surface. To tailor the properties of BST, surface modifications may be performed, such as thin film deposition, surface functionalization, or chemical treatments. This modification can introduce additional layers or coating on the surface, leading to different morphology and interface characteristics.





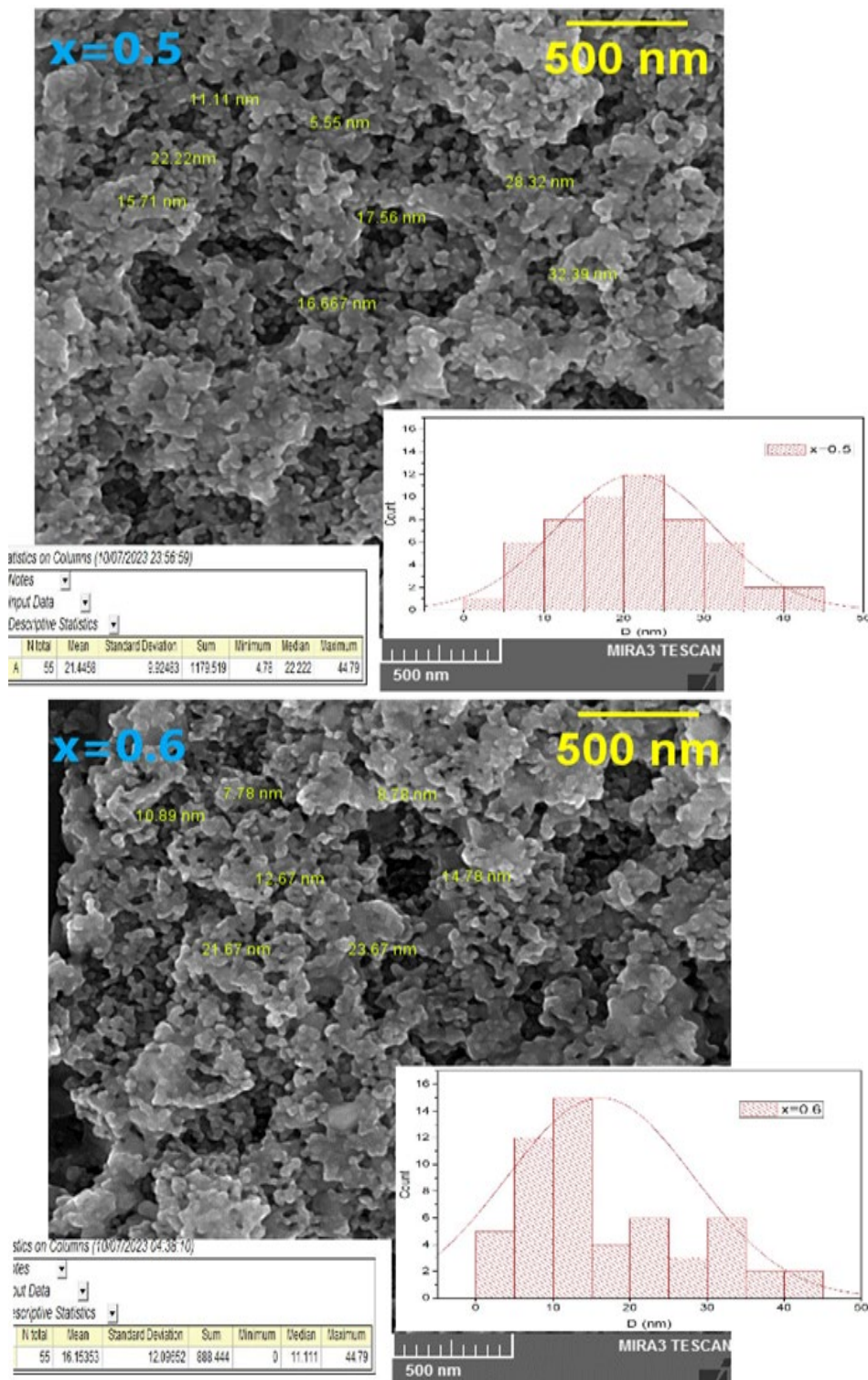


Fig. 1. FESEM images for $Ba_{1-x}Sr_xTiO_3$ thin film with different ratios of x .

The sol-gel technique was used to manufacture $Ba_{1-x}Sr_xTiO_3$ powders with different x values. Figure 2 illustrates the structures of these powders. The experiment revealed that each of the samples exists in a polycrystalline state by default. The diffraction peaks move to higher angles as the amount of Sr^{+2} ions in a material rises. This shows that the phase structure changes from tetragonal to cubic. Afterwards, the value of x increases from $x = 0.2$ to $x = 0.6$. As the Ba

concentration increases in BST, the diffractive angle decreases, or the inter-planar separation (d) shown in Table 1 increases.

The change in ionic radius can influence the crystal structure of $Ba_{1-x}Sr_xTiO_3$. The substitution of Sr^{2+} ions may lead to distortions or changes in the symmetry of the crystal lattice, which can be detected through modifications in the XRD pattern. These changes may manifest as shifts or broadening of the diffraction peaks, indicative of structural disorder or lattice strain.

In the case of $Ba_{1-x}Sr_xTiO_3$, the substitution of Sr^{2+} for Ba^{2+} can lead to changes in the preferred orientation of the crystal domains, which can be discerned through variations in the intensities of the XRD peaks. This increase in ionic radius can lead to a gradual expansion of the unit cell and an increase in the lattice parameters, such as the unit cell volume or the lattice constant.

The introduction of different-sized ions into a crystal lattice can induce lattice strain or disorder, leading to peak broadening in XRD patterns. This broadening arises due to variations in interatomic distances and local distortions caused by the size mismatch between Ba and Sr ions.

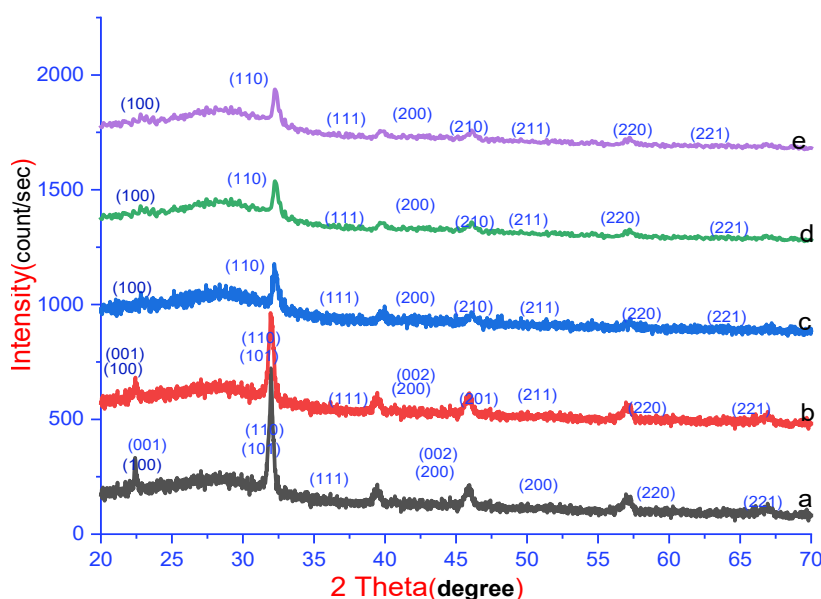


Fig. 2. XRD pattern of $Ba_{1-x}Sr_xTiO_3$ thin film with different values of x ($a=0.2$, $b=0.3$, $c=0.4$, $d=0.5$, $e=0.6$).

Table 1. The d -interspace and Miller indices for $Ba_{1-x}Sr_xTiO_3$ phases.

X ratio	"x=0.2"	"x =0.3"	"x =0.4"	"x =0.5"	"x =0.6"
d-Theoretical	3.9890	3.977	3.9660	3.9494	3.9394
d-experimental	3.9893	3.9771	3.9600	3.9470	3.9390
(hkl)	(101)/(100)	(101)/(100)	(100)	(100)	(100)
Phases	Tetragonal	Tetragonal	Cubic	Cubic	Cubic
No PDF card	96-151-2121	00-044-0039	00-034-0411	00-039-1395	01-078-2723

BST exhibits a perovskite crystal structure, which consists of a three-dimensional network of corner-sharing TiO_6 octahedra. $Ba_{1-x}Sr_xTiO_3$ is a solid solution consisting of Ba and Sr ions substituted for each other in the crystal lattice and by varying the x ratio, the composition of the film changes, leading to various structural and morphological properties.

$Ba_{1-x}Sr_xTiO_3$ is known to exhibit a perovskite crystal structure [5]. As the strontium content varies (x changes), the material may undergo phase transitions. These transitions can influence the arrangement of atoms and alter the electrical properties, including conductivity. The impact of Sr^{+2} ions on Barium strontium titanate conductivity (BST) is substantial due to the solid solution behavior

of the materials. The introduction of Sr^{+2} ions into the BaSrTiO_3 crystal lattice leads to changes in the electronic and structural properties, affecting the overall electrical conductivity.

The substitution of Sr^{+2} instead of Ba^{+2} ions in $\text{Ba}_{1-x}\text{Sr}_x\text{TiO}_3$, as the Sr^{+2} content (x) increases in $\text{Ba}_{1-x}\text{Sr}_x\text{TiO}_3$ leads to increasing conductivity on the BST compound as shown in Fig. 3. Due to Sr^{+2} having more electrons than barium then the result is to add electrons into the crystal structure. This increase in the concentration of charge carriers such as electrons enhances the electrical conductivity of the materials. As the Sr content (x) increases in $\text{Ba}_{1-x}\text{Sr}_x\text{TiO}_3$, more strontium ions with extra electrons are incorporated into the lattice, leading to a higher concentration of electron carriers and an increase in electrical conductivity.

Understanding these effects is crucial for tailoring the electrical properties of $\text{Ba}_{1-x}\text{Sr}_x\text{TiO}_3$ for specific applications in electronics, capacitors, sensors, and other functional devices.

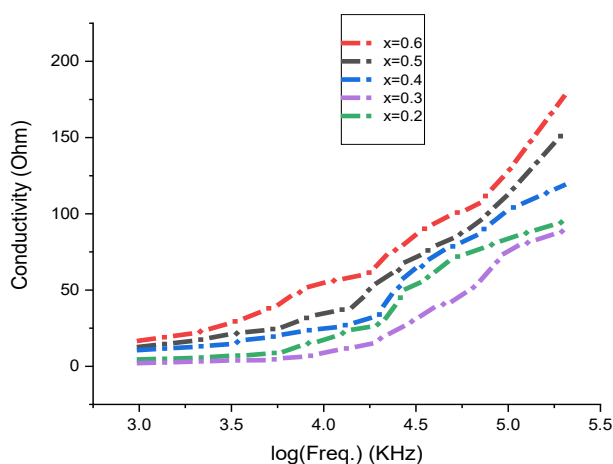


Fig. 3. The conductivity of BaSrTiO_3 versa the ratio value of x .

It is essential to carefully control the annealing process for BST to optimize its electrical conductivity. The specific relationship between annealing temperature and conductivity for $\text{Ba}_{1-x}\text{Sr}_x\text{TiO}_3$ may vary depending on annealing temperatures as shown in Fig. 4. Researchers and engineers typically conduct systematic studies to identify the optimal annealing conditions to achieve the desired conductivity for their specific applications and at high temperatures; it can lead to significant grain growth. Larger grains with fewer grain boundaries can enhance the overall electrical conductivity because electrons encounter fewer obstacles as they move through the material. As a result, the conductivity of BST tends to increase with increasing annealing temperature up to a certain point.

While high-temperature annealing can reduce certain defects and improve conductivity, excessive annealing temperatures can introduce new defects or lead to the loss of certain elements (e.g., oxygen vacancies), which can adversely affect the conductivity. Annealing can cause changes in the concentration of oxygen vacancies within the material. Oxygen vacancies can act as charge carriers, and their concentration can affect the electrical conductivity of $\text{Ba}_{1-x}\text{Sr}_x\text{TiO}_3$. Higher annealing temperatures can lead to larger grain sizes, reducing the number of grain boundaries and defects. This can improve the electrical conductivity by facilitating smoother charge carrier transport through the material.

Generally, in the case of $\text{Ba}_{1-x}\text{Sr}_x\text{TiO}_3$, as the annealing temperature increases, the electrical conductivity tends to improve due to enhanced crystallinity, reduced defects, and increased dopant activation [2]. However, it is crucial to note that there is an optimal annealing temperature range for each specific composition (x value) of $\text{Ba}_{1-x}\text{Sr}_x\text{TiO}_3$ and exceeding this range might lead to undesired effects such as grain growth and phase separation.

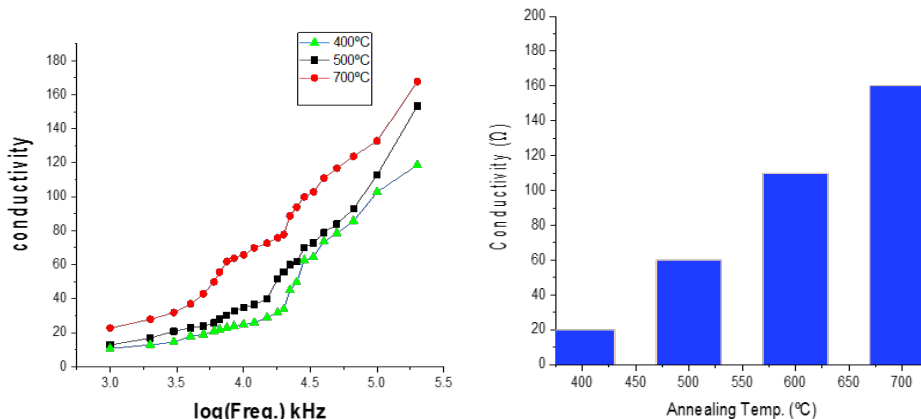


Fig. 4. The annealing temperature versus conductivity of $Ba_{1-x}Sr_xTiO_3$, $Ba_{0.6}Sr_{0.4}TiO_3$ model.

In Fig. 5, BST films' dielectric constant as a function of frequency at varied parameters and x concentrations. Up to 50 kHz, the dielectric constant decreases slightly and then remains constant. For frequencies above 50 kHz, interfacial/surface polarization contributes less to the dielectric constant than electronic, ionic, dipolar, and interfacial/surface polarization. The frequency determines the total polarization from mechanism contributions. They contribute at low frequencies and disappear at higher frequencies because of relaxation.

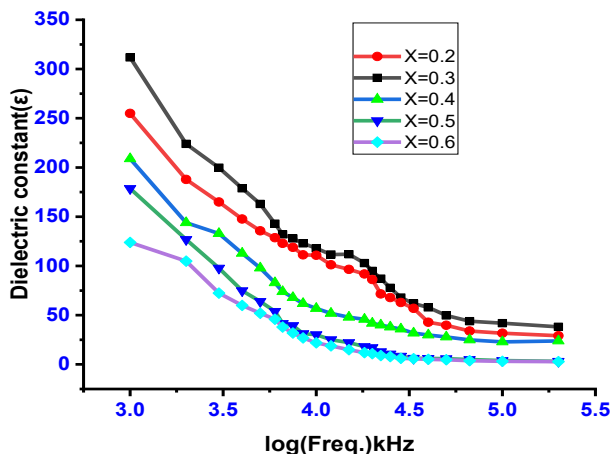


Fig. 5. The dielectric constant versus frequency with different values of x.

The dielectric constant versus temperature is shown in Fig. 6. It decreases with increased temperature, so increases the conductivity of BST films. The reason was the increasing conductivity of the film due to the vibration of the atoms or molecules around their sites, so the vibration led to the exciting of atoms and may increase the responsible charge carriers.

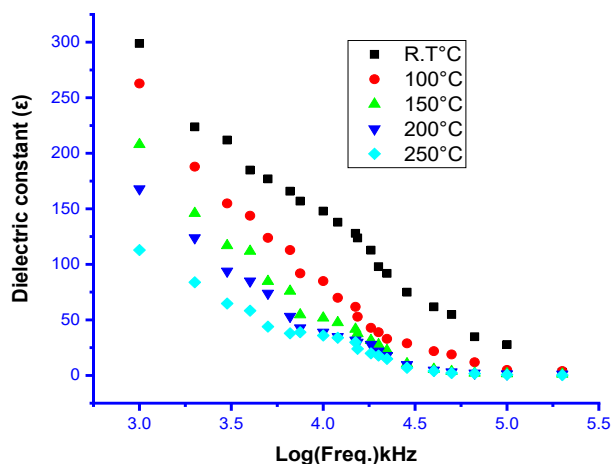


Fig. 6. The dielectric constant versus frequency with different temperatures.

6. Conclusion

The above study showed that there is a significant effect of the ion radius on the structural and electrical properties of ferroelectric materials such as perovskite BaSrTiO₃. The X-ray diffraction analysis confirmed the formation phases of Ba_{1-x}Sr_xTiO₃ depend on x values. The XRD pattern exhibited the phase change from the tetragonal phase to the cubic phase when the values of x increased. The ion radius affected the morphology of the film and the particle size of the film. The average particle size changes with the ratio of x, the particle size varied with the values of x increased as revealed by the Field Emission Scanning Electron Microscope. The results show that as the ion radius varies, the crystal structure undergoes distortions, affecting the symmetry and stability of the BaSrTiO₃ thin films. Electrical properties change depending on the change in particle size, The conductivity of BST films increased with increasing frequency and with increased temperatures. The annealing temperature also affects the conductivity, the annealing temperature increases due to an increase in the dielectric constant. The dielectric constant decreased with increasing frequency.

Acknowledgments

I wish to acknowledge thankful to Al-Shatrah University in Iraq and all the staff who helped me to achieve my work.

References

- [1] S. M. K. Hamed A Gatea, Int. J. Mod. Phys. B, 38(14), p. 2450175, (2024).
- [2] S. Uddin, A. Ali, A. Zaman, H. Alrobei, A. H. Alghtani, V. Tirth, A. Algahtani, F. Ullah, Digest Journal of Nanomaterials and Biostructures, 17(3), p.793-798, (2022); <https://doi.org/10.15251/DJNB.2022.173.793>
- [3] P. Kirthika, N. Thangaraj, P. Anitha, Journal Ovonic research, 19(2),(2023); <https://doi.org/10.15251/JOR.2023.192.231>
- [4] H. A. G. Omer A. Alawi, Aziz Ibrahim Abdulla, Sustain. Energy Technol. Assessments, 49, (2022).
- [5] H. A. Gatea, S. J. Shoja, H. J. Albazoni, Jom, 75(11), pp. 4470-4478, (2023); <https://doi.org/10.1007/s11837-023-06052-6>
- [6] A. K. Bain, Ferroelectr. Lett. Sect., 34(5-6), pp. 149-154, (2007); <https://doi.org/10.1080/07315170701759017>

- [7] H. Seo et al., *J. Appl. Phys.*, 107(2), pp. 0-7, (2010)
- [8] H. A. Gatea, S. J. Shoja, H. J. Albazoni, *J. Ovonic Res.*, 19(4), pp. 379-386, (2023); <https://doi.org/10.15251/JOR.2023.194.379>
- [9] H. A. Gatea, H. Abbas, I. S. Naaji, *Int. J. Thin Film Sci. Technol.*, 11(2), (2022)
- [10] H. A. Gatea, S. M. Khalil, *Eur. Phys. J. D*, 76(8), (2022); <https://doi.org/10.1140/epjd/s10053-022-00462-y>
- [11] H. A. Gatea, *J. Mater. Sci. Mater. Electron.*, 34(6), (2023); <https://doi.org/10.1007/s10854-023-09860-3>
- [12] M. M. Hameed, S. A. Aldaghfag, M. Saeed, *Journal of Ovonic Research*, 19(5), p. 513 - 523 (2023); <https://doi.org/10.15251/JOR.2023.195.513>
- [13] Rusiyanto et al., *Int. J. Automot. Mech. Eng.*, 18(2), pp. 8752-8759, (2021).
- [14] E. A. R. Assirey, *Saudi Pharm. J.*, 27(6), pp. 817-829, (2019); <https://doi.org/10.1016/j.jsps.2019.05.003>
- [15] H. A. Gatea, *J. Phys. Conf. Ser.*, 1829(1), pp. 0-7, (2021); <https://doi.org/10.1088/1742-6596/1829/1/012030>
- [16] H. A. Gatea, H. Abbas, M. L. Shaghnab, *ECS J. Solid State Sci. Technol.*, 12(8), p. 083002,(2023); <https://doi.org/10.1149/2162-8777/acec11>
- [17] N. Zhang et al., *Coatings*, 11(12), pp. 3-11, (2021); <https://doi.org/10.3390/coatings11111316>
- [18] E. Yecue, H. Laysandra, D. Triyono, *J. Phys. Conf. Ser.*, 1442(1), pp. 1-5, (2020); <https://doi.org/10.1088/1742-6596/1442/1/012020>
- [19] R. Dewi, Krisman, Zulkarnain, Rahmawati, T. S. L. S. Husain, *AIP Conf. Proc.*, 2169, November, pp. 0-6, (2019)
- [20] A. Setiawan, E. K. Palupi, R. Umam, H. Alatas, Irzaman, *Ferroelectrics*, 568(1), pp. 62-70, (2020); <https://doi.org/10.1080/00150193.2020.1735893>